

$^3\text{He } A \rightarrow B$ Transition in Finite Geometries

Peter Kostädt and Mario Liu

Institut für Theoretische Physik, Universität Hannover, 30167 Hannover, Germany

PACS. 67.50F - Superfluid phase

PACS. 68.10J - Kinetics

Abstract. - The measured and reported rate [1] of the $^3\text{He } A \rightarrow B$ transition depends on the diameter of the experimental cell. Theoretically, this can only be explained by a direct drag on the interface exerted by the lateral walls, leading to a pressure discontinuity across the interface. This has not been considered before, either here or in similar circumstances. The general hydrodynamic theory that includes the influence of finite geometries is presented.

Introduction. - General hydrodynamic considerations [2–4] on the ^3He $A \rightarrow B$ transition have in the past yielded a fairly complete picture for the infinite geometry. Depending on the interface velocity \dot{u} , there are two qualitatively different types of behavior. If \dot{u} is small compared to the second-sound velocity, $\dot{u} \ll c_2$, three characteristic features of the *phase coherent transition* are predicted: (i) The chemical potential is continuous across the interface, forcing the melting A phase to be warmer than the growing B phase. (ii) The relevant mode of heat transfer, second sound, is efficient enough to obliterate any onset of hypercooling. (iii) The effective growth resistance preventing the transition rate to diverge consists of three elements in series: two account for the sq-mode, a hydrodynamically gentle temperature variation on each side of the interface, the third accounts for a sharp temperature discontinuity at the microscopically narrow interface. The former two dissipative elements stem from collisions among quasiparticles, the latter one (probably much smaller in magnitude) results from Andreev scattering of these particles at the interface. At the fast end of the transition, $\dot{u} \gg c_2$, circumstances are rather different: (i) Second sound is now a comparatively slow process, leaving the chemical potential discontinuous and the growing B phase warmer, since an ever-increasing portion of the latent heat is no longer removed from the interface region. (ii) The usual scenario of hypercooling (in which no heat at all is transferred) becomes asymptotically valid. (iii) The total growth resistance contains both additive and multiplicative contributions.

Since second sound is so important in determining the properties of the A - B transition, it seems plausible that the above features would not easily survive in a confining geometry: walls hold back the normal velocity v_n and thus confine the range of heat transfer via second sound. In what follows we briefly state what this range is, why its finiteness is important, and that it alone is insufficient to account for the measured [1] geometry dependence of the phase transition. Generally, for stationary flows, lateral walls are well-accounted for by a relaxation term $\rho v_n / \tau$ in the Navier-Stokes equation (obtained by averaging over the cross section of the experimental cell, eg. $\tau = \rho R^2 / 8\eta$ for a cylinder of radius R). As a result of this term, the second-sound step functions sent out by the moving interface [2–4] acquire

an extra, exponentially decaying factor. In the rest frame of the interface, with B phase at $x < 0$ and A phase at $x > 0$, it is $\exp(x/\lambda_2)$. The resulting stationary temperature profile is shown in Fig. 1 and 2. (On the scale of these figures, the temperature variations of the sq- and diffusive modes [4] are too small to be separated from the discontinuity at the interface, $x = 0$.) The decay length

$$\lambda_2 = -\rho_n \tau (c_2^2 - \dot{u}^2) / (\rho_s \dot{u}) \quad (1)$$

is also the range of heat transfer via second sound. Outside this range, $|x| \gg |\lambda_2|$, there is no means for heat transfer, and energy balances locally. Now, it is important to realize that the usual thermodynamic consideration of hypercooling is based on local balance of energy. Hence, the temperature $T^B = T^A + \delta T$ of the growing B phase is taken to be given by the A phase temperature T^A and the heating δT from the released latent heat. Second sound transfers heat away from the interface and invalidates this consideration. However, if the heat transfer has a finite range, hypercooling remains a valid concept outside this range. And indeed, Fig. 1 shows that the B phase is warmer than the A phase for $x \gg |\lambda_2|$. In addition, the solution depicted in Fig. 1 is obtained under the condition

$$\left[|\Delta\mu| - (\Delta\sigma)^2 / \partial_T \sigma^B \right]_{T=T_i} \geq 0, \quad (2)$$

which is, up to first order in $T_{AB} - T_i$, equivalent to the usual and approximative hypercooling condition $(T_{AB} - T_i) - l_{AB}/c \geq 0$. (T_i : initial undercooling temperature; T_{AB} : coexistence temperature; μ : chemical potential, σ : entropy, l_{AB} : latent heat, c : specific heat, all per unit mass; Δ : difference across the interface, eg. $\Delta\mu \equiv \mu^B - \mu^A$.)

Above the hypercooled region, $\varepsilon \equiv 1 - T_i/T_{AB} \lesssim 0.5\%$, planar instability and non-stationarity (the usual conundrum of snow flakes) may be expected to be relevant, but are not: Approaching the critical value $\varepsilon_c \sim 0.5\%$ from below, \dot{u} vanishes with the left side of Eq. (2), and λ_2 diverges accordingly. Once λ_2 exceeds the longitudinal dimensions of the experimental cell, even a heat transfer within the scale of λ_2 is sufficient to disturb the energy balance and invalidate the concept of hypercooling. Then a planar transition becomes viable

again. (The appropriate solution is non-stationary, similar to that of Ref. [2]; see discussion at the end of the introduction.)

Concentrating now on the hypercooled region, where the stationary solutions of Fig. 1 and 2 are valid, we nevertheless face the following difficulty: Despite the relaxation term $\rho v_n/\tau$ and the resulting qualitatively changed behavior of second sound, the interface velocity \dot{u} remains independent of the cell radius R , in stark contrast with the well-documented experimental observations [1]. This is indeed perplexing, since the hydrodynamic description accounts for the structure of the dynamics and is independent of specific mechanisms, especially if any has been overlooked. Re-examining the equations of Ref. [2–4], we found no reason to doubt the strict conservation of energy and mass, leaving the momentum as the only candidate to resolve the puzzle: Rough lateral walls break the translational symmetry and it is conceivable that the Navier-Stokes equation acquires a relaxation term that is singular at the interface, resulting in a discontinuity of the momentum current,

$$\Delta p = \Gamma \rho \dot{u} / R . \quad (3)$$

This equation can be viewed as the equation of motion for the interface, in which the inertial term $\sim \ddot{u}$ and the restoring force $\sim u$ vanish; the pressure discontinuity Δp is the external force (per unit area), while the damping $\sim \dot{u}$ comes from the drag exerted by the lateral walls and would have its origin, for instance, in the interaction between the surface tension (including textural contributions) and the wall’s roughness. The total drag should be proportional to the contact length, $2\pi R$ in a cylinder, per unit area it is $\sim 1/R$. Γ is introduced as a phenomenological parameter, accounting for the degree of roughness. As we shall see, Eq. (3) indeed establishes agreement between theory and experiment. More specifically, we find a “wall contribution” $\sim 1/R$ added to the total growth resistance of the infinite geometry, so that the change of \dot{u} is also proportional to $1/R$. (The necessity of having $\Delta p \neq 0$ has not arisen before, such as at the well-studied ^4He II-vapor or ^4He II-solid interfaces [5]. At least, it was not studied there. A re-examination may be worthwhile.)

Finally, we address the relationship between the stationary solution of second sound

presented here and the propagating step functions of Ref. [2–4] in the case of an infinite geometry. It is noteworthy that letting $R \rightarrow \infty$, the exponentially decaying solution does not reduce to the same steps. This is because of the following reasons: In deriving the stationary solution here, the lateral dimension is taken to be finite, the longitudinal one infinite; and although an arbitrarily large R results in an arbitrarily large decay length λ_2 , it is finite and always smaller than the longitudinal dimension. The energy current Q in the present solution is constant, it always is in stationary, one-dimensional solutions, $\partial_x Q = -\partial_t e \equiv 0$. Since Q vanishes outside λ_2 (aside from a constant equilibrium contribution) it must also vanish within [6]. This alone is enough to exclude the type of solution represented by the step functions propagating toward infinity, all the while transferring energy. The two types of solutions are in fact mutually exclusive: If the lateral geometry is confining enough to entail a decay length λ_2 much smaller than the longitudinal dimension, the stationary solution presented here is relevant, while the propagating solution is valid in the opposite, open limit, where the λ_2 is much larger than the longitudinal dimension.

Theory. - In what follows, we shall derive the general stationary solution of superfluid hydrodynamics for the temperature T , the counterflow velocity $w \equiv \rho_s(v_n - v_s)/\rho_n$ and the A - B interface velocity \dot{u} , taking into account the relaxation term $\rho v_n/\tau$ in the momentum conservation, and the altered connecting condition, Eq. (3). The solutions for T and w we search for are stationary in the rest frame of the interface, with the B phase at $x < 0$ and the A phase at $x > 0$. Before the actual calculation, however, we need to point out the following consideration that significantly simplifies our task: As long as the radius of the experimental cell is not too small, $R \gtrsim 0.1\text{cm}$, the physics close to the interface, especially the sq- and the diffusive lengths, are little changed from the infinite geometry, and most of the results from Ref. [4] remain valid and need not be recalculated. More specifically, we have three characteristic length scales: (i) The microscopic width of the interface, too small to be considered in a hydrodynamic approach except as the location of discontinuities. (ii) The large decay length of second sound, Eq. (1), $\lambda_2 \approx -\lambda_R c_2/\dot{u}$ for $\dot{u} \ll c_2$ and $\lambda_2 \approx \lambda_R \dot{u}/c_2$ for $\dot{u} \gg c_2$, where the characteristic length $\lambda_R \equiv \tau c_2 \rho_n/\rho_s$ is of order 0.1cm for radii $R \sim 0.1\text{cm}$.

(iii) The mesoscopic decay lengths of various exponential functions. Although individually describable in a hydrodynamic theory, they may also be collectively accounted for by a total growth resistance of an effective interface [4] (that is wide enough to include these decays). The decay lengths are the sq-length λ_{sq} for $\dot{u} \ll c_2$ and the diffusive lengths λ_T^D , λ_w^D for $\dot{u} \gg c_2$. In an infinite geometry, all three are combinations of two characteristic lengths, both of order 10^{-2}cm : $\lambda_T \equiv k/(2c_2\rho T\partial_T\sigma)$ and $\lambda_w \equiv [(4/3)\eta - \rho(\zeta_1 + \zeta_4) + \zeta_2 + \rho^2\zeta_3]\rho_s/(2\rho\rho_n c_2)$. (The heat conductance k and the viscosities η , ζ_{1-4} are defined in the usual way [7], neglecting anisotropy.) In a finite geometry, the mesoscopic decay lengths are modified in first order of λ_T/λ_R , λ_w/λ_R as

$$\lambda_{sq}^{A,B} = 2(\lambda_T\lambda_w)^{1/2} \left(1 \mp \frac{\lambda_T + \lambda_w}{2(\lambda_T\lambda_w)^{1/2}} \frac{\dot{u}}{c_2} - \frac{\lambda_T}{\lambda_R - \lambda_T} \right) \quad (4)$$

and

$$\lambda_T^D = 2\lambda_T \frac{c_2}{\dot{u}} \left(1 - \frac{2\lambda_T}{\lambda_T - \lambda_w} \frac{\lambda_T}{\lambda_R} \frac{c_2^2}{\dot{u}^2} \right), \quad \lambda_w^D = 2\lambda_w \frac{c_2}{\dot{u}} \left(1 + \frac{2\lambda_w}{\lambda_T - \lambda_w} \frac{\lambda_w}{\lambda_R} \frac{c_2^2}{\dot{u}^2} \right). \quad (5)$$

The correction terms obviously may be safely neglected for radii $R \gtrsim 0.1\text{cm}$. For this experimentally relevant case (the only one we study [8]), we may therefore take the effective interface as calculated in Ref. [4] for the infinite geometry, especially the total growth resistance, and only consider the change further away from the interface, on length scales of λ_R . (Technically, this allows us to discard all dissipative terms in the hydrodynamic equations except the new relaxation term $\rho v_n/\tau$, cf. the detailed discussion on the effective interface in Ref. [4].)

Linearizing the averaged hydrodynamic equations with respect to $w \equiv \rho_s(v_n - v_s)/\rho$ and $T^{A,B} - T_i$, and retaining terms of second order in \dot{u}/c_2 and c_2/\dot{u} respectively, the stationary solution for $\dot{u} \ll c_2$ is given by

$$T^B(x) = T_i + \delta T^B, \quad T^A(x) = T_i + \delta T_2^A \exp\left(-\frac{\dot{u}}{c_2} \frac{x}{\lambda_R}\right), \quad (6a)$$

$$w^B(x) = 0, \quad w^A(x) = \delta w_2^A \exp\left(-\frac{\dot{u}}{c_2} \frac{x}{\lambda_R}\right), \quad (6b)$$

and for $\dot{u} \gg c_2$ by

$$T^B(x) = T_i + \delta T^B + \delta T_2^B \exp\left(\frac{c_2}{\dot{u}} \frac{x}{\lambda_R}\right), \quad T^A(x) = T_i, \quad (7a)$$

$$w^B(x) = \delta w_2^B \exp\left(\frac{c_2}{\dot{u}} \frac{x}{\lambda_R}\right), \quad w^A(x) = 0. \quad (7b)$$

As discussed above, second-sound and the related energy transfer now acquires a finite range. Its decay length $\lambda_2 = -\lambda_R(c_2^2 - \dot{u}^2)/(c_2\dot{u})$ is negative for $\dot{u} < c_2$ and positive for $\dot{u} > c_2$. (Therefore, $\delta T_2^B, \delta w_2^B = 0$ in the first and $\delta T_2^A, \delta w_2^A = 0$ in the second case.) In a confined geometry, the amplitudes of the stationary second-sound modes are related by

$$\delta w_2^{A,B} = \dot{u} (\partial_T \sigma / \sigma) \delta T_2^{A,B} \quad (8)$$

(in contrast to the well-known relation $\delta w_2^{A,B} = \pm c_2 (\partial_T \sigma / \sigma) \delta T_2^{A,B}$ for the infinite geometry). The constant δT^B accounts for the temperature rise due to the latent heat and the interface dissipation, while $\delta T^A = 0$ due to causality and the lack of any means for long range energy transfer. The temperature fields (outside the effective interface), are plotted in Fig. 1. and 2.

The interface velocity \dot{u} and the independent amplitudes of Eqs. (6), (7) are to be determined from the general connecting conditions (CCs) at the effective interface:

$$\Delta Q = 0, \quad \Delta g = 0, \quad \Delta p = \Gamma \rho \dot{u} / R, \quad (9)$$

$$\Delta(\mu + v_n v_s) = 0, \quad R_s = \langle f \rangle \Delta T + g \Delta \mu. \quad (10)$$

All quantities are defined in the rest frame of the interface and have been averaged over the cross section of the experimental cell. The mass current is given as $g = -\rho \dot{u}$ [2,4], $\langle f \rangle$ denotes the average $\frac{1}{2}(f^B + f^A)$ of the entropy current across the interface. Except the non-vanishing discontinuity of the pressure p , all CCs are as derived in Ref. [4], though the subscript e for “effective” has been eliminated from Δ and $\langle \rangle$. From the derivation there, it is also clear that R_s is the total entropy production within the effective interface. The entropy produced by the drag exerted by the lateral walls at the rate of $\dot{u} \Delta p = \Gamma \rho \dot{u}^2 / R$ is therefore implicitly included in R_s . Subtracting this part, one obtains the rate of entropy produced in an infinite geometry

$$R_s^\infty = R_s - \Gamma \rho \dot{u}^2 / R , \quad (11)$$

which was parametrized as $R_s^\infty = \langle f \rangle^2 / \kappa_e$ and g^2 / K_e , respectively for $\dot{u} \ll c_2$ and $\dot{u} \gg c_2$; cf. [2]. (Explicit expressions for the effective, R -independent Onsager coefficients κ_e , K_e can be found in Ref. [4].) Since the term $\Gamma \rho \dot{u}^2 / R$ in Eq. (11) can be rewritten as $\Gamma \langle f \rangle^2 / (R \rho \langle \sigma \rangle^2)$ and $\Gamma g^2 / (R \rho)$, we finally obtain from $R_s \sim \langle f \rangle^2$ and g^2 the CC:

$$\langle f \rangle = \left(\kappa_e^{-1} + \Gamma / (R \rho \langle \sigma \rangle^2) \right)^{-1} \Delta T \quad \text{and} \quad (12)$$

$$g = \left(K_e^{-1} + \Gamma / (R \rho) \right)^{-1} (\Delta \mu_o + \langle \sigma \rangle \Delta T) , \quad (13)$$

respectively for $\dot{u} \ll c_2$ and $\dot{u} \gg c_2$. Here, μ_o denotes the chemical potential for given pressure and temperature, in a system with $v_n = v_s = 0$.

Expanding the CCs to first order in the deviation from the initial temperature T_i , we obtain a set of equations for the interface velocity \dot{u} and the amplitudes δT^B , δT_2^A (or δw_2^B).

In the limit of $\dot{u} \ll c_2$, it is solved by

$$\delta T^B = - \left[\frac{\Delta \sigma}{\partial_T \sigma^B} + \frac{\Delta \mu_o + \Gamma \dot{u} R^{-1}}{T \partial_T \sigma^B} \right]_i , \quad (14a)$$

$$\delta T_2^A = \delta T^B - \left[\frac{1}{\sigma^A} \left(\frac{(\Delta \sigma)^2}{\partial_T \sigma^B} + \Delta \mu_o + \Gamma \dot{u} R^{-1} \right) \right]_i , \quad (14b)$$

$$\dot{u} = - \left(\frac{\rho \langle \sigma \rangle_i}{\kappa_e} + \frac{2\Gamma}{R} \right)^{-1} \left[\frac{(\Delta \sigma)^2}{\partial_T \sigma^B} + \Delta \mu_o \right]_i , \quad (14c)$$

while the dependent counterflow amplitude is given as $\delta w_2^A = \dot{u} [\partial_T \sigma^A / \sigma^A]_i \delta T_2^A$. Note the R -dependence of the constant temperature δT^B , caused by the drag $\sim \Gamma$. Since \dot{u} is taken to be positive here (melting the A phase on the right), the validity of Eqs. (14) is confined to initial temperatures satisfying $[|\Delta \mu_o| - (\Delta \sigma)^2 / \partial_T \sigma^B]_i \geq 0$, cf. the discussion in the introduction. For $\dot{u} \gg c_2$, expansion of the CCs around T_i and linearization with respect to c_2 / \dot{u} , δT^B and δw_2^B lead to

$$\delta T^B = - \left[\frac{\Delta \sigma}{\partial_T \sigma^B} + \frac{\Delta \mu_o + \Gamma \dot{u} R^{-1}}{T \partial_T \sigma^B} \right]_i , \quad (15a)$$

$$\delta w_2^B = - \left[\frac{\rho_s \Delta \mu_o + \Gamma \dot{u} R^{-1} - \sigma^B \delta T^B}{\rho_n \dot{u}} \right]_i , \quad (15b)$$

$$\dot{u} = - \left(\frac{\rho}{K_e} + \frac{2\Gamma}{R} \right)^{-1} \left[\Delta \mu_o - \frac{1}{2} \Delta \sigma \delta T^B \right]_i , \quad (15c)$$

while the dependent temperature amplitude is given as $\delta T_2^B = (1/\dot{u})[\sigma^B/\partial_T \sigma^B]_i \delta w_2^B$. Again, δT^B contains an R -dependent contribution from the latent heat and the interface entropy-production R_s ; cf. Eq. (14a).

Summary. - The influence of finite geometries is considered, the interface velocity \dot{u} and the stationary temperature field are derived. For both $\dot{u} \ll c_2$ and $\dot{u} \gg c_2$, the total growth resistance of the transition is a sum of the open geometry Onsager-coefficient and a “wall contribution” $\sim \Gamma/R$. Hence \dot{u} (for given T_i) is maximal for $R \rightarrow \infty$, as measured [1]. The phenomenological parameter Γ depends on the cell’s inner surface, cf. Eq. (3). Two sets of \dot{u} , obtained in tubes of different radii R , should suffice to determine Γ . This is not possible with the published data [1], however, because the tubes used were made of different materials, copper and epoxy, with presumably rather different Γ . Perhaps further experimentals will fill this gap.

Defining a total growth coefficient as $K_{tot}(T_i/T_{AB}, H) \equiv (1/K_e + 2\Gamma/R\rho)^{-1}$, we estimate from the data of Ref. [1] that $K_{tot}(0.81, 1.5\text{kOe}) = 1.9 \text{ g s cm}^{-4}$, $K_{tot}(0.81, 3.0\text{kOe}) = 2.8 \text{ g s cm}^{-4}$, $K_{tot}(0.85, 1.5\text{kOe}) = 1.3 \text{ g s cm}^{-4}$, $K_{tot}(0.85, 3.0\text{kOe}) = 1.4 \text{ g s cm}^{-4}$; obviously, K_{tot} increases with increasing magnetic field or decreasing supercooling rate.

A paper containing the algebraic details of this letter and of Ref. [4] is being prepared.

Acknowledgment. - One of the authors (P.K.) acknowledges financial support of the Deutsche Forschungsgemeinschaft (DFG).

REFERENCES

- [1] D. S. Buchanan, G. W. Swift, and J. C. Wheatley, Phys. Rev. Lett. **57**, 341 (1986); S. T. P. Boyd and G. W. Swift, Phys. Rev. Lett. **64**, 894 (1990); J. Low Temp. Phys. **86**, 325 (1992) and **87**, 35 (1992).
- [2] M. Grabinski and M. Liu, Phys. Rev. Lett. **65**, 2666 (1990).
- [3] P. Panzer and M. Liu, Phys. Rev. Lett. **69**, 3658 (1992); J. Low Temp. Phys. **92**, 127 (1993);
- [4] P. Kostädt and M. Liu, Phys. Rev. Lett. **71**, 3513 (1993);
- [5] B. Castaing and P. Nozières, J. Phys. (Paris) **41**, 701 (1980); H. Wiechert, J. Phys. C: Solid State Phys. **9**, 553 (1976); H. Wiechert and F. I. Buchholz, J. Low Temp. Phys. **39**, 623 (1980) and **51**, 291 (1993); S.E. Korshunov, Zh. Eksp. Teor. Fiz. **92**, 1320 (1987) [Sov. Phys. JETP **65**, 741 (1987)]; M. Grabinski and M. Liu, J. Low Temp. Phys. **73**, 79 (1988);
- [6] The non-equilibrium part of Q vanishes only in the interface system, where we have $\partial_x Q = 0$ in the bulk, $\Delta Q = 0$ at the interface, and $Q(x) = Q_{equil}$ for $x \gg |\lambda_2|$, hence $Q(x) = Q_{equil}$ also for $x \lesssim |\lambda_2|$. (For clarity, we confine the formula to the limit $\dot{u} \ll c_2$.) In the laboratory system, we still have $\partial_x Q = 0$ in both phases, but the connecting condition is now $\Delta Q = -\rho \dot{u} l_{AB}$, and the above conclusion does not hold. Rather, the correct picture here is the heating up of the A phase, within λ_2 , by redistributing the latent heat l_{AB} via second sound.
- [7] D. Vollhardt and P. Wölfe, *The Superfluid Phases of Helium 3*, Taylor and Francis, London (1990).
- [8] Obviously, the assumption $v_n = 0$ in the original calculation of Leggett and Yip becomes valid for radii $R \ll 0.1\text{cm}$; cf. A. J. Leggett and S. K. Yip, in *Helium Three* (eds. W. P. Halperin and L. P. Pitaevskii), Modern Problems in Condensed Matter Sciences, Vol. 26, p. 523, North-Holland, Amsterdam (1990); A. J. Leggett, J. Low Temp. Phys. **87**, 571 (1992).

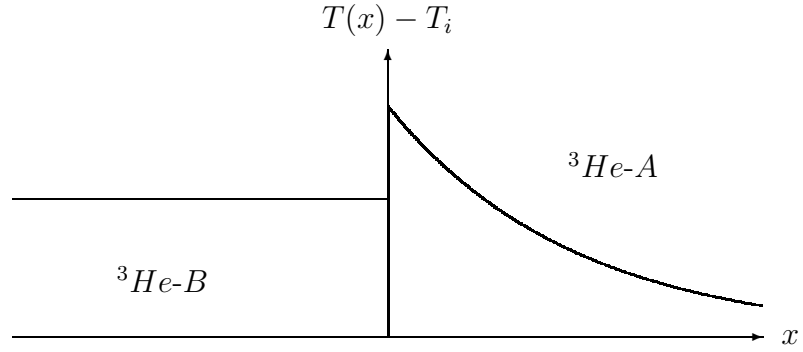


FIG. 1. The temperature field for $\dot{u} \ll c_2$, as in Eq. (6a).

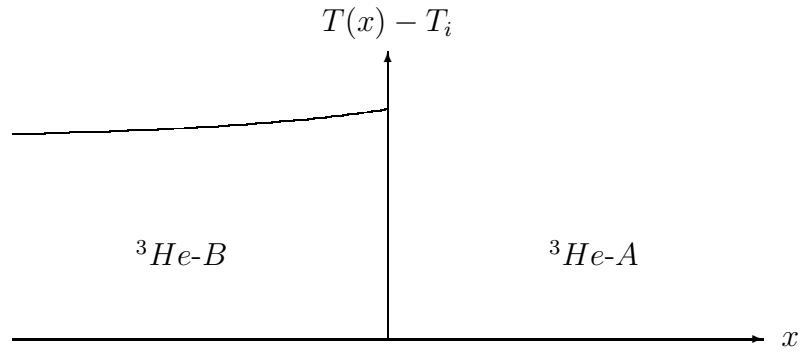


FIG. 2. The temperature field for $\dot{u} \gg c_2$, as in Eq. (7a).